REMOVAL OF CRYSTAL VIOLET FROM AQUEOUS SOLUTION USING BAMBOO BIOCHAR

Đến tòa soạn: 21-05-2025

Đinh Thuy Van[1], Pham Viet Linh[2], Nguyen Thi To Loan[1], Ngo Thi Mai Viet[1*]

1. Chemistry Faculty, Thai Nguyen University of Education
2. 11th-grade French class, Thai Nguyen Specialized High School

**E-mail: vietntm@tnue.edu.vn*

TÓM TẮT

HẤP PHỤ TÍM TINH THỂ TRÊN THAN SINH HỌC CHẾ TẠO TỪ CÂY TRE

Bài báo này trình bày các kết quả nghiên cứu về khả năng loại bỏ tím tinh thể trong môi trường nước của than sinh học chế tạo từ cây tre. Một số đặc trưng hóa lí của than trước và sau khi hấp phụ tím tinh thể được nghiên cứu bằng phương pháp kính hiển vi điện tử quét (SEM), phổ tán sắc năng lượng tia X (EDX), đo diện tích bề mặt riêng (BET), quang phổ hồng ngoại (FT-IR) và đo điện thế zeta. Điều kiện tối ưu cho quá trình hấp phụ tím tinh thể trên vật liệu là: pH 10; thời gian tiếp xúc pha 90 phút; khối lượng vật liệu 0,10 gam/ thể tích dung dịch tím tinh thể là 25 mL; lực ion từ 1 - 10 mM NaCl. Sự hấp phụ tím tinh thể trên vật liệu tuân theo mô hình đẳng nhiệt Langmuir và Freundlich. Quá trình hấp phụ tím tinh thể trên vật liệu là quá trình tự xảy ra và thu nhiệt. Bước đầu chứng minh cơ chế hấp phụ tím tinh thể trên than sinh học cây tre chịu sự ảnh hưởng của lực tương tác tĩnh điện và không tĩnh điện.

Từ khóa: *Hấp phụ, tím tinh thể, than sinh học cây tre, mô hình đẳng nhiệt.*

1. INTRODUCTION

Dyes are widely used in various industrial sectors, and their discharge into the environment has emerged as a critical ecological concern. Among these, crystal violet (CV) is frequently employed in the paper and wood processing industries and is also a constituent in inks and ballpoint pens. Furthermore, CV possesses antimicrobial, antifungal, and antiviral properties, making it applicable in medical and pharmaceutical contexts [1]. However, CV was known to exhibit cytotoxic and genotoxic effects, posing significant risks to cells upon direct contact, particularly epithelial cells of the skin and mucosal linings of the gastrointestinal tract [2,3]. Consequently, the removal of CV from wastewater was imperative to mitigate its environmental and health impacts. Adsorption garnered considerable attention as a remediation strategy due to its advantages, including low operational cost, high removal efficiency, simplicity in design and operation, as well as environmental sustainability [4–8]. In this study, biochar derived from bamboo was investigated as an effective adsorbent for the removal of CV from aqueous solutions, leveraging its cost-effectiveness, environmental compatibility, and favorable physicochemical properties. CV, being a cationic dye in aqueous media, could be efficiently removed through interaction with the functional groups and porous structure of bamboo-derived biochar.

2. EXPERIMENTS

2.1. Chemicals and Equipment

2.1.1. Chemicals

- Bamboo biochar was purchased from

Tachibana Bamboo Co. Ltd (Japan).

- CV, which was analytical reagent, were collected from Guangdong Guanghua Chemical Factory (China).

- HCl 37 %, NaOH ≥ 97 % and NaCl ≥ 99,5 % were purchased from Merck (Germany).

2.1.2. Equipment

UV-1700 spectrophotometer (Shimadzu, Japan); 4-digit electronic balance, Presisa XT 120A (Switzerland); 2-digit pH meter, Presisa 900 (Switzerland); drying oven, Jeitech (Korea); H4Y shaker and 80-2 centrifuge (China).

2.2. Study on the factors affecting the adsorption process

Effect of pH (Experiment 1):

A 25.0 mL sample of CV solution with a concentration of 25.00 mg/L was added to a series of 100 mL Erlenmeyer flasks, each containing 0.05 g of the adsorbent material. The pH of the dye solutions was adjusted to range from 3.0 to 10.0 using 0.1 M HCl and 0.1 M NaOH solutions. The mixtures were shaken on a shaker for 150 minutes at 300 rpm at room temperature (30 ± 2 °C).

Effect of Material Mass:

The effect of material mass on dye adsorption capacity was investigated in a manner similar to those written in *Experiment 1*. The pH of the CV solution was adjusted to the optimized value, and the material mass was varied from 0.01 g to 0.14 g.

Effect of Contact Time:

The effect of contact time on dye adsorption capacity was examined using the same procedure as decribed in *Experiment 1*, with the previously optimized pH and material mass. The contact times studied were 5, 10, 30, 60, 90, 120, 150, and 180 minutes.

Effect of Ionic Strength:

The effect of ionic strength on dye adsorption capacity was examined by introducing the strong electrolyte NaCl, and was assessed similarly to those written in *Experiment 1*. The concentration of CV was kept constant in NaCl solutions with concentrations ranging from 0 mM to 100 mM, under optimized pH, material mass, and contact time conditions.

Effect of Temperature:

The effect of temperature on the dye adsorption capacity of the material was investigated similarly to those written in *Experiment 1*, using the optimized pH, material mass, and contact time. The temperatures examined ranged from 30 °C to 70 °C.

Effect of CV Concentration:

In 0 mM NaCl solution:

The effect of CV concentration on dye adsorption in a 0 mM NaCl solution was studied following the same procedure as described in *Experiment 1*, using the optimized pH, material mass, and contact time. The concentrations of CV tested were 25.00, 50.00, 100.00, 300.00, 400.00, and 500.00 mg/L.

In 5 mM NaCl solution:

Similarly, the effect of CV concentration on dye adsorption in a 5 mM NaCl solution was evaluated using a similar procedure and conditions. The concentrations of CV used were 25.00, 50.00, 100.00, 300.00, 400.00, and 500.00 mg/L.

Equation (1) represents the formula for calculating the adsorption capacity of CV: $q = \frac{(C_0 - C_{cb})}{m}.V$ (1)

where: C_o và C_{cb} are the initial and equilibrium concentrations of CV solution before and after adsorption, respectively (mg/L); q is the adsorption capacity (mg/g); m is the mass of the adsorbent material (g).

The adsorption efficiency of crystal violet is calculated using the formula (2):

$$H = \frac{(C_0 - C_{cb})}{C_0} . 100\ \% \qquad (2)$$

where: Co và Ccb are the initial and equilibrium concentrations of CV solution before and after adsorption, respectively (mg/L); H is the adsorption efficiency (%).

The concentration of crystal violet was determined by molecular absorption spectrophotometry.

2.3. Study on the adsorption isotherm models

The data on the effect of initial dye concentration on CV adsorption capacity were analyzed using the Langmuir and Freundlich isotherm models to study the adsorption behavior of CV on the material.

2.4. Study on the adsorption thermodynamics

To evaluate the thermodynamic parameters of the adsorption process, the adsorption capacity of crystal violet at different temperatures was analyzed, and the Van't Hoff equation (3) was applied to calculate the thermodynamic parameters.

$$LnK_D = -\frac{\Delta G^0}{RT} = -\frac{\Delta H^0}{RT} + \frac{\Delta S^0}{R} \qquad (3)$$

where K_D is the equilibrium constant derived from the relationship between the equilibrium concentrations of CV in the solution and its adsorption capacity; R is the universal gas constant (8.314 $J.mol^{-1}.K^{-1}$); T is the temperature (K); ΔG^0 is the standard Gibbs free energy change ($kJ.mol^{-1}$); ΔS^0 is the entropy change ($kJ.mol^{-1}.K^{-1}$), and ΔH^0 is the enthalpy change ($kJ.mol^{-1}$).

2.5. Preliminary Study on the Adsorption Mechanism

The adsorption mechanism of CV (crystal violet) on bamboo biochar was initially investigated based on the results of adsorption isotherm studies, as well as analyses of the material's characteristics after CV adsorption using FT-IR spectroscopy and zeta potential measurements.

3. RESULTS AND DISCUSSION

3.1. Physicochemical Characteristics of the Material

The synthesized bamboo-derived biochar was systematically characterized to elucidate its physicochemical properties. Scanning electron microscopy (SEM) analysis (Figure 1a) revealed a highly porous architecture with uniformly distributed honeycomb-like cavities, indicative of structural evolution during the pyrolysis process. This thermal decomposition of volatile organic constituents during pyrolysis contributed to the development of the observed porous morphology. Brunauer–Emmett–Teller analysis (Figure 1b) determined a specific surface area of 332.90 m²/g, which was relatively high and suggests substantial adsorption capacity. The large surface area was considered a key factor enhancing the biochar's performance in adsorbing crystal violet from aqueous solutions.

The energy-dispersive X-ray spectroscopy analysis of bamboo-derived biochar, as illustrated in Figure 1c, revealed the presence of carbon (C), oxygen (O), magnesium (Mg), silicon (Si), phosphorus (P), and potassium (K). Notably, carbon constitutes the predominant element, accounting for 86.02% of the total composition. This substantial carbon content was indicative of the material's high surface area and porous structure, which were critical factors contributing to its efficient adsorption capacity for crystal violet in aqueous solutions.

Zeta potential analysis revealed a negative surface charge of −27.9 mV (Figure 1d), indicating the presence of surface functional groups that contributed to electrostatic interactions with cationic contaminants. The distribution and nature of these functional groups were strongly influenced by pyrolysis parameters, particularly temperature and residence time.

Fourier-transform infrared spectroscopy was employed to elucidate the surface functional groups. As illustrated in Figure 1e, the broad absorption band typically associated with the O–H stretching vibration of crystalline water (3600–3200 cm^{-1}) was absent following pyrolysis, suggesting the effective removal of moisture and alteration of hydroxyl functionalities [9]. Notably, absorption bands observed at 1650 cm^{-1} and 2187 cm^{-1} were indicative of carbonyl (C=O) and carboxyl (–COOH) groups, respectively [10], which were commonly associated with enhanced adsorption capacity.

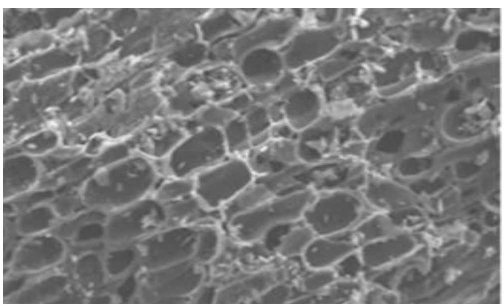

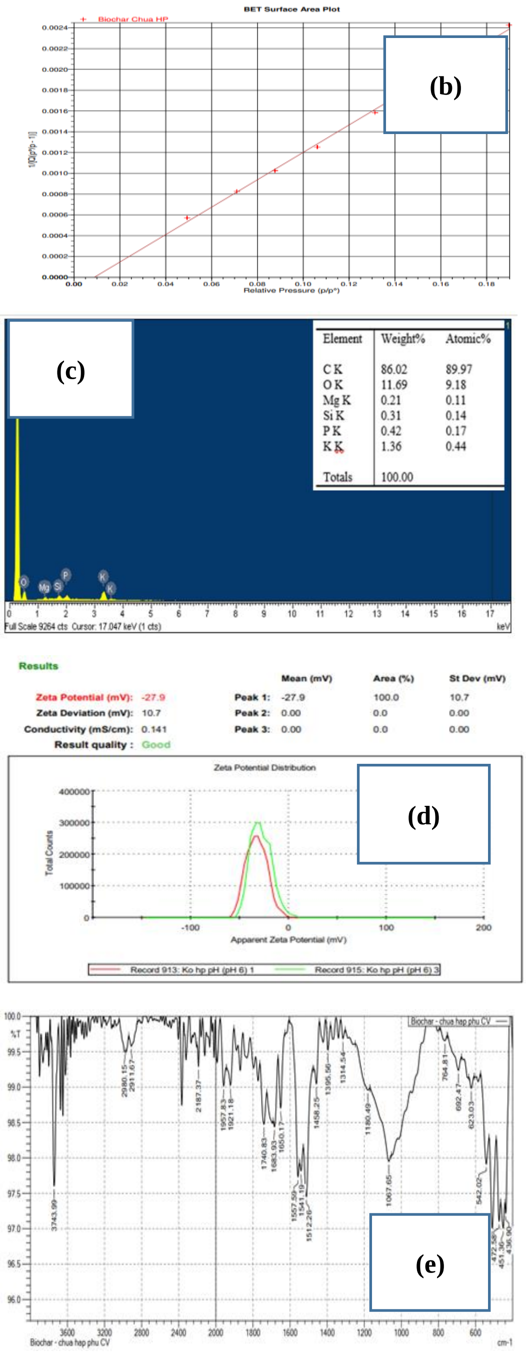

Figure 1. *Some physicoche… characteristics of bamboo biochar… EDX (b), zeta potential (pH 6) (c), B… d FT-IR (e)*

Integrative characterization via SEM, BET, EDX, zeta potential and FT-IR analyses confirmed that the bamboo biochar possesses a porous morphology, high carbon content, and surface functionalities comprising carbonyl and carboxyl groups. The combination of these structural and chemical attributes, along with its negatively charged surface, positions bamboo biochar as a promising candidate for the adsorption of cationic pollutants such as crystal violet.

3.2. Effects of Operational Parameters on Crystal Violet Adsorption

Figures 2 presented the effects of operational parameters-including solution pH, adsorbent dosage, contact time, ionic strength, and temperature-on the adsorption efficiency removal of crystal violet using bamboo biochar.

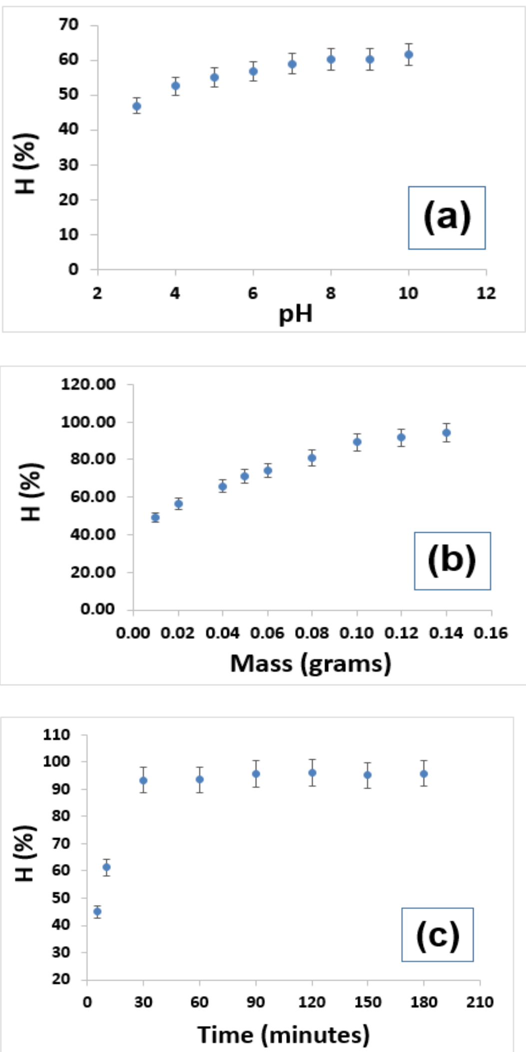

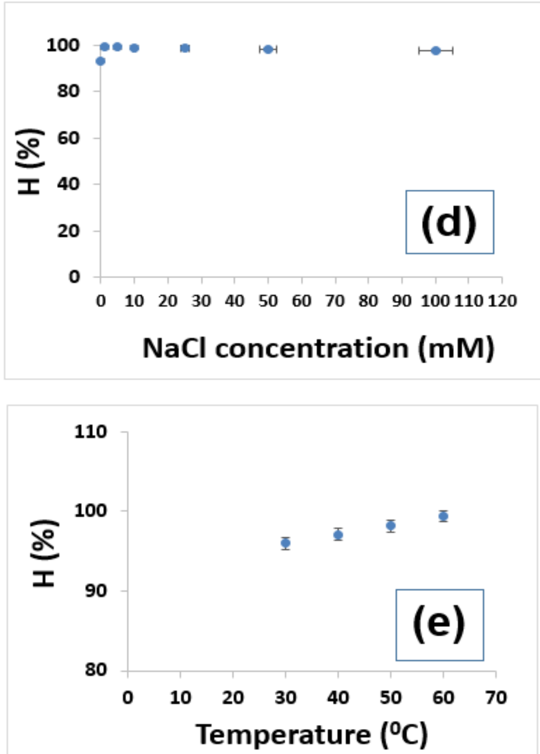

Figure 2. *The effect of pH (a), mass (b), time (c), ionic strength (d), and temperature (e) on the adsorption efficiency of CV*

As can be seen in Figure 2a, the highest adsorption efficiency of CV on the material occurred at pH 10. This could be explained by the fact that CV existed in a cationic form in solution; therefore, in acidic pH regions, competitive adsorption might occur between the dye cations and H^+ ions, resulting in lower adsorption efficiency. At higher pH levels, conditions were favorable for the adsorption of dye cations onto the negatively charged surface of the material. At pH values above 10, the increased viscosity of the solution adversely affected the adsorption efficiency. Consequently, pH levels greater than 10 were excluded from the investigation. Therefore, pH 10 was selected as the optimal value for subsequent experiments. The optimal pH for the adsorption of CV on bamboo biochar was consistent with that observed for adsorption on rice husk biochar and modified rice husk biochar [11].

Figure 2b showed that as the mass of the material increased from 0.01 grams to 0.10 grams, the adsorption efficiency of CV increased rapidly. This could be attributed to the rapid increase in available adsorption sites with increasing material mass. However, at higher masses, the increase in adsorption efficiency became insignificant. Therefore, a material mass of 0.10 grams was used for subsequent studies.

As illustrated in Figure 2c, when the contact time increased from 5 to 30 minutes, the adsorption efficiency of CV by the material rose rapidly. From 30 to 90 minutes, adsorption efficiency increased more slowly and remained nearly constant at later time points. Based on these results, 90 minutes was selected as the equilibrium adsorption time for the next experiments.

Figure 2d showed that the adsorption efficiency of CV on bamboo biochar was influenced by ionic strength. Specifically, in the presence of a NaCl solution, the adsorption efficiency increased compared to when NaCl was absent. Moreover, the efficiency reached a peak (approximately 99%) at low NaCl concentrations (1–10 mM) and decreases slightly at medium to high concentrations (25–100 mM).

The results on the effect of temperature on the adsorption efficiency of CV (Figure 2e) showed that as the temperature increased, the adsorption efficiency of CV on bamboo biochar also increased.

3.3. Adsorption Isotherm Models

The influence of initial dye concentration on the adsorption capacity of crystal violet was investigated under two conditions: without ionic strength and in the presence of 5 mM NaCl. The equilibrium data obtained were fitted to the Langmuir and the Freundlich isotherm models to elucidate the adsorption behavior. The corresponding results were summarized in Figure 3 and Table 1.

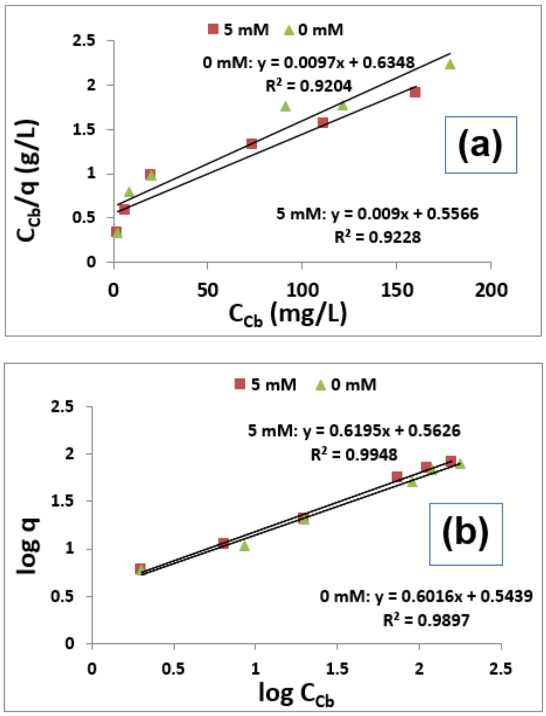

Figure 3. *Adsorption isotherm models fitted to the experimental data: (a) Langmuir isotherm; (b) Freundlich isotherm*

Table 1. Adsorption parameters based on the Langmuir and Freundlich isotherm models

Parameters / $C_{M\ NaCl}$	Langmuir model			Freundlich model		
	q_{max} (mg/g)	R^2	b (L/mg)	n	R^2	k
0 mM	103.09	0.920	0.015	1.66	0.989	3.49
5 mM	111.11	0.922	0.016	1.61	0.994	3.65

The adsorption behavior of crystal violet (CV) onto bamboo biochar was better described by the Freundlich isotherm model than by the Langmuir model, indicating a heterogeneous adsorption surface. The maximum adsorption capacities estimated from the Langmuir isotherm were 103.09 mg/g and 111.11 mg/g in the absence and presence of 5 mM NaCl, respectively.

The maximum adsorption capacity of CV on bamboo biochar and other materials was presented in Table 2.

Table 2. Adsorption capacity of CV on different materials

Materials	Adsorption capacity (mg/g)	Experimetal conditions	Ref.
Modified rice husk	90.02	pH 10; 0.025 g; 70 mins; 25 mL of dye	11
Activated Carbons Prepared from Rice Husk	64.87	pH 10.8; 0.4 g; 120 mins; 200 mL of dye	12
Orange peel Biochar	203.81 (25°C) 223.88 (40°C)	pH 9; 12 hours; 50 mL of dye	13
Palm Kernel Shell-Derived Biochar	24.45	pH 10; 0.5 g; 24 hours; 30 mL of dye	14
Bamboo biochar	103.09 (0mM NaCl) 111.11 (5mM NaCl)	pH 10; 0.1 g; 90 mins; 25 mL of dye	This study

As presented in Table 2, the adsorption capacity of CV onto bamboo biochar was lower than that of orange peel biochar; however, it was markedly higher than that of the other materials. These findings highlighted the significant potential of bamboo biochar as an efficient adsorbent for the removal of dye pollutants from aqueous solutions.

3.4. Adsorption Thermodynamics

By processing experimental data on the effect of temperature on the adsorption capacity of CV using the Van't Hoff equation, we obtained the results shown in Figure 4 and Table 3.

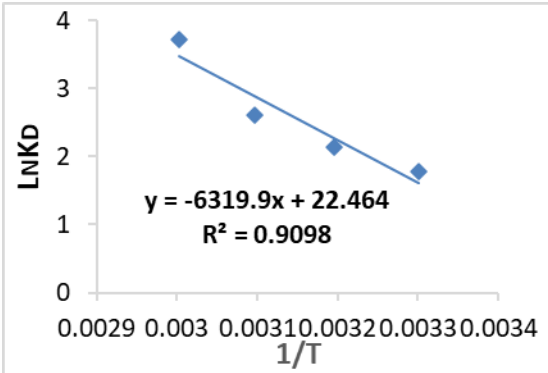

Figure 4. *Dependence of LnK_D on the value of 1/T*

From the equation representing the dependence of LnK_D on 1/T, the values of ΔG^0, ΔH^0, and ΔS^0 were calculated and were presented in Table 3.

Table 3. *Thermodynamic parameters*

T (^{0}C)	ΔG^0 (kJ.mol^{-1})	ΔH^0 (kJ.mol^{-1})	ΔS^0 (kJ.mol^{-1}.K^{-1})
30	-4.497	52.543	0.186
40	-5.551		
50	-7.010		
60	-10.330		

The negative values of the standard Gibbs free energy change (ΔG^0) and the positive values of the standard enthalpy change (ΔH^0) indicated that the adsorption of CV onto the material was a spontaneous and endothermic process. This behavior was consistent with the adsorption of CV onto activated carbon-impregnated fabric, as reported in previous studies [15]. Furthermore, the increasingly negative ΔG^0 values at higher temperatures suggested that the adsorption process became more thermodynamically favorable as the temperature increases.

3.5. Proposed adsorption mechanism

Based on the physicochemical characterization results of the material after CV adsorption (Figure 5), a plausible adsorption mechanism of CV onto the material could be proposed.

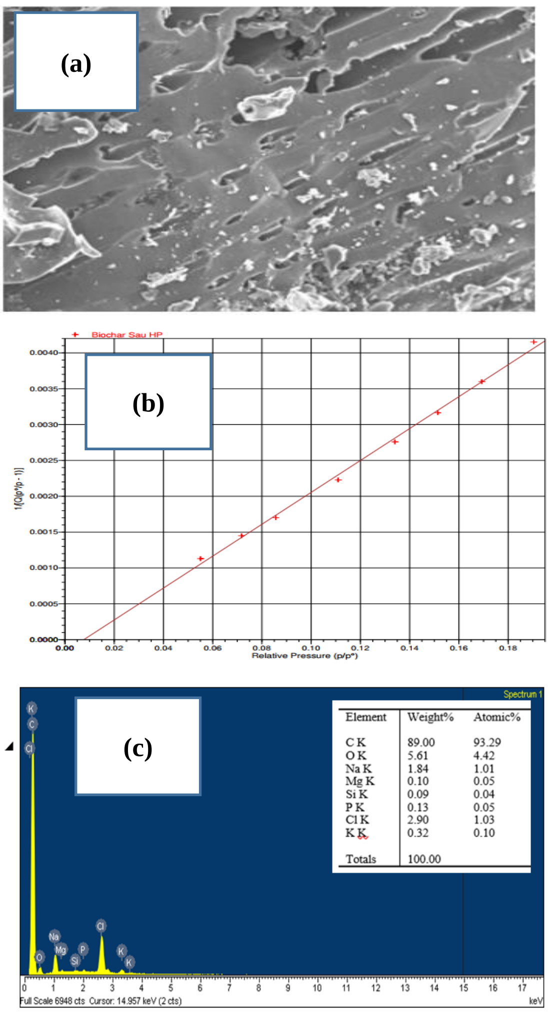

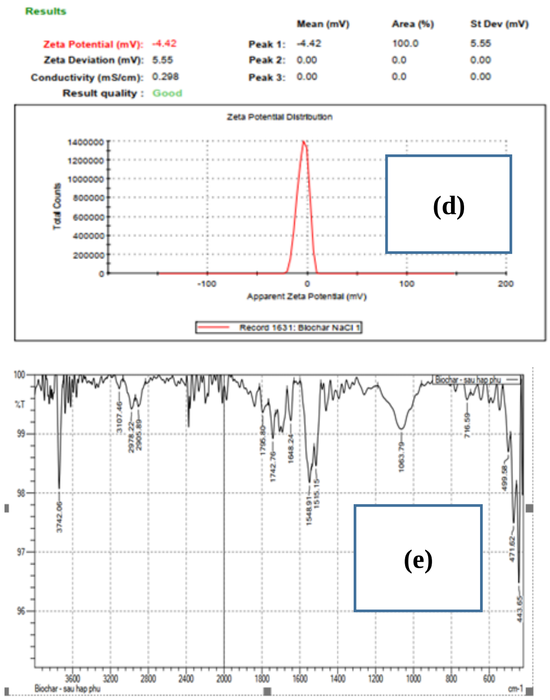

Figure 5. Some physicochemical characteristics of bamboo biochar after CV adsorption: SEM (a), EDX (b), zeta potential (pH 6) (c), BET (d), and FT-IR (e)

The SEM image (Figure 5a) of the biochar after CV adsorption revealed a significant reduction in porosity compared to the pristine material. Correspondingly, the specific surface area decreased markedly from 332.90 m²/g to 197.16 m²/g (Figure 5b). This notable decline in surface area suggested that CV molecules were effectively adsorbed onto the material, occupying and blocking the pore structures and thereby reducing the available surface area of the material.

The EDX spectrum of bamboo-derived biochar was shown in Figure 5c. Analysis indicated that, in addition to the primary elements C, O, Mg, Si, P, and K, the biochar after CV adsorption also contained Cl (2.90%) and Na (1.84%). The presence of Cl was attributed to CV, while Na originated from the NaOH solution used for pH adjustment during the adsorption process. Furthermore, the carbon content of the biochar increased from 86.02% to 89.00% post-adsorption, whereas the oxygen content decreased from 11.69% to 5.61%, suggesting changes in surface chemistry associated with the adsorption of crystal violet. The zeta potential of the material after CV adsorption (Figure 5d) became less negative (−4.42 mV) compared to that of the pristine material (−27.9 mV), indicating a reduction in surface charge negativity. This shift suggested that cationic dye molecules were adsorbed onto the material surface primarily via electrostatic interactions.

The FT-IR spectrum of the biochar after CV adsorption (Figure 5e) exhibited a characteristic peak at 1063.79 cm^{-1}, which could be assigned to the C–N stretching vibration within the crystal violet (CV) molecule. Moreover, the absorption band observed at 2978.22 cm^{-1} corresponded to the asymmetric stretching vibration of methylene ($–CH_2$) groups, while the peak at 1648.24 cm^{-1} was attributed to the C=C stretching vibration of the aromatic ring structure [16].

Thus, the SEM, EDX, zeta potential, BET and FT-IR analysis results of bamboo biochar, both before and after CV adsorption, demonstrated that the dye was successfully adsorbed onto the material. The FT-IR and zeta potential analyses also showed that the adsorption of CV onto bamboo biochar was influenced by electrostatic interactions between the CV cations and the negatively charged surface of the material, as well as by hydrophobic interactions between the CV molecules and the organic functional groups of the material. The adsorption mechanism of CV onto bamboo biochar was similar to that of another organic compound, ciprofloxacin antibiotic, onto the same material [17].

4. CONCLUSION

The physicochemical properties of bamboo-derived biochar were characterized by SEM, BET, EDX, zeta potential and FT-IR. The biochar exhibited a porous structure, high carbon content, carboxyl functional groups, and a relatively large surface area. Optimal adsorption conditions for CV were pH 10, 90 min contact time, 0.10 g biochar per 25 mL dye solution, and ionic strength of 1–10 mM NaCl. Adsorption efficiency increased with temperature, indicating a spontaneous and endothermic process. The adsorption followed the Freundlich isotherm model more closely than the Langmuir model, with a maximum capacity of 103.09 mg/g and 111.11 mg/g in the absence and presence of 5 mM NaCl, respectively. Post-adsorption analyses (SEM, BET, EDX, zeta potential and FT-IR) confirmed successful dye removal driven by both electrostatic and non-electrostatic interactions.

Commitment: I hereby affirm that this is our original work and that its content has not been submitted to any other journal for publication.

REFERENCES

[1] Maley, Alexander M.; Arbiser, Jack L, (2013). Gentian Violet: a 19th century drug re-emerges in the 21st century, Experimental Dermatology, **12(22)**, 775–780.

[2] W Au, M A Butler, S E Bloom, T S Matney, (1979). Further study of the genetic toxicity of gentian violet, *Mutation Research/Genetic Toxicology,* **2(66)**, 103-112.

[3] W Au, S Pathak, C J Collie, T C Hsu, (1978). Cytogenetic toxicity of gentian violet and CV on mammalian cells in

vitro. *Mutation Research/Genetic Toxicology*, **2-3(58),** 269-276.

[4] Abdolmaleki, A., Mohamadi, Z., & Bazyar, Z., (2024). A simple, efficient, and rapid method for dye removal from wastewater using an IDA-GO@Fe_3O_4 magnetic nanocomposite. *RSC Advances*, **14**, 27843-27851.

[5] Vasundra Nagendran, et al., (2025). Challenges and advances in nanocellulose-based adsorbents for dye removal: mechanisms and future directions. *Discover Applied Sciences*, **7:14**.

[6] Nguyen Thi Tuyet Nhi, Nguyen Thi Mai Tho, Nguyen Thi Hong Anh, (2024). An efficient adsorbent for the removal of dyes prepared by an in situ growth of ZIF-8 onto activated carbon. *Environmental Technology & Innovation, Green Chemistry Letters and Reviews*, **1(17),** 1-16.

[7] Dahlan, I., Abdul Aziz, H., & Hung, Y.-T, (2024). Recent development of metal-organic framework 5 adsorbents for organic dye removal from aqueous solution. *International Journal of Environment and Waste Management*, **3(35).**

[8] Joanna Kyziol- Komosinska, et al., (2024). Compost as Green Adsorbent for the Azo Dyes: Structural Characterization and Dye Removal Mechanism. *Korean Journal of Chemical Engineering*, **41,** 3227–3243.

[9] He, S., Wu, L., Zeng, Y., Jia, B., Liang, L., (2022). Preparation of Ce-Ag Bimetallic Modified Biochar Composite for the Efficient Removal of Sulfathiazole and its Mechanism. *Materials Today Communications*, **(33)**, 104577.

[10] Sahoo, S.S., Vijay, V.K., Chandra, R., Kumar, (2021). Production and characterization of biochar produced from slow pyrolysis of pigeon pea stalk and bamboo, H.J.C.E.. *Technology*, **3**, 100101.

[11] Puspa Lal Homaga, et al., (2022). Adsorption and removal of crystal violet dye from aqueous solution by modified rice husk. *Heliyon*, **8**.

[12] Kaustubha Mohanty, et al., (2006). Removal of Crystal Violet from Wastewater by Activated Carbons Prepared from Rice Husk,. *Ind. Eng. Chem. Res.*, **45**, 5165-5171.

[13] Tang, L., et al., (2025). Efficient adsorption of crystal violet by different temperature pyrolyzed biochar-based sodium alginate microspheres: A green solution for food industry dye removal. *Food Chemistry: X*, **26**, 102311.

[14] Phyo Phyo Kyi, et al., (2020). The Removal of Crystal Violet from Textile Wastewater Using Palm Kernel Shell-Derived Biochar. *Appl. Sci. 2020*, **10**, 2251.

[15] Batuhan Mulla, et al., (2024). Removal of Crystal Violet Dye from Aqueous Solutions through Adsorption onto Activated Carbon Fabrics. *Journal of Carbon Research*, **1**(**10)**, 1-18.

[16] Thi Mai Viet Ngo, et al., (2020). Surface Modified Laterite Soil with an Anionic Surfactant for the Removal of a Cationic Dye (Crystal Violet) from an Aqueous Solution. *Water Air Soil Pollution*, 231:285**.**

[17] Tien Duc Pham, et al., (2023). Adsorption characteristics of ciprofloxacin and naproxen from aqueous solution using bamboo biochar. *Biomass Conversion and Biorefinery*, **11**.